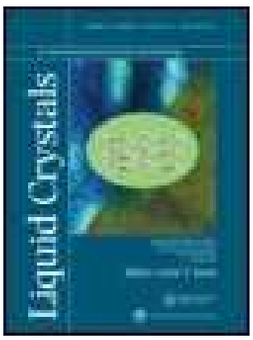

Liquid Crystals

ISSN: 0267-8292 (Print) 1366-5855 (Online) Journal homepage: http://www.tandfonline.com/loi/tlct20

An experimental and computational study of calamitic and bimesogenic liquid crystals incorporating an optically active [2,2]-paracyclophane

Richard J. Mandle & John W. Goodby

To cite this article: Richard J. Mandle & John W. Goodby (2018): An experimental and computational study of calamitic and bimesogenic liquid crystals incorporating an optically active [2,2]-paracyclophane, Liquid Crystals, DOI: 10.1080/02678292.2018.1453559

To link to this article: https://doi.org/10.1080/02678292.2018.1453559

LIQUID CRYSTALS, 2018
https://doi.org/10.1080/02678292.2018.1453559

Taylor & Francis
Taylor & Francis Group

An experimental and computational study of calamitic and bimesogenic liquid crystals incorporating an optically active [2,2]-paracyclophane

Richard J. Mandle and John W. Goodby

Department of Chemistry, University of York, York, UK

ABSTRACT

Two liquid-crystalline materials containing an optically active (R)-4-hydroxy-[2,2]-paracyclophane group were prepared, one in which the chiral group is a bulky terminal unit and one in which it forms part of a terphenyl-like mesogenic unit. Both materials exhibit monotropic chiral nematic phases. Partial phase diagrams were constructed for mixtures of both materials with 5CB, allowing us to extrapolate pitch lengths and helical twisting power values (HTP) for each material. The HTP value of the material with a 'locked' paracyclophane is 70% higher than that of a 'free' paracyclophane and this is rationalised as being due to the reduction in conformational freedom of the former material relative to the later.

ARTICLE HISTORY
Received 25 January 2018
Accepted 13 March 2018

KEYWORDS
Liquid Crystal; Planar Chirality; Chirality; Dimer; Cholesteric; Helical Twisting Power; cyclophane

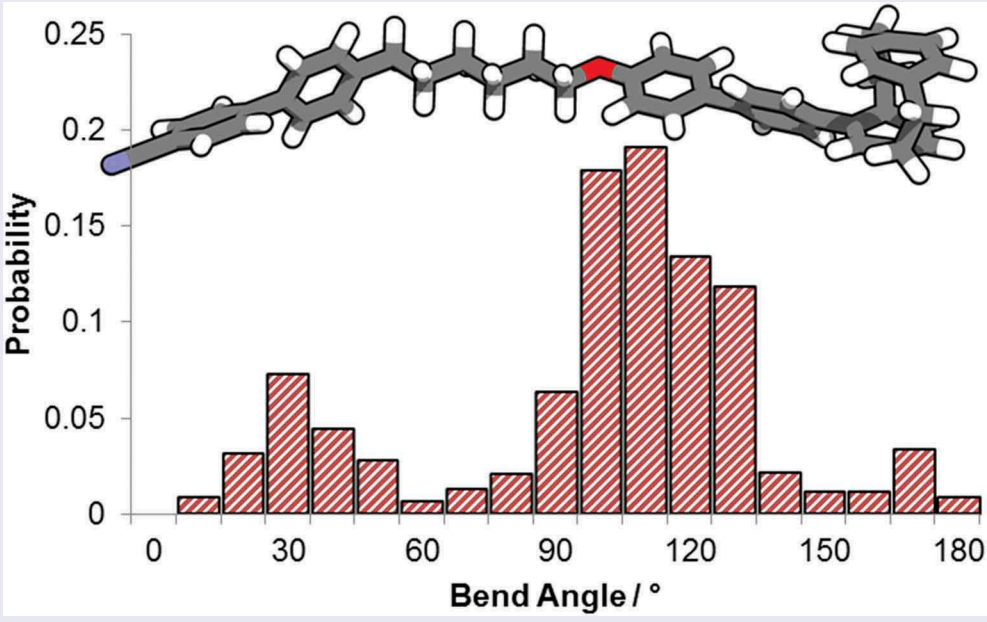

Introduction

There are three types of chirality relevant to chemistry and molecular structure; point chirality (*e.g.* citronellol), axial chirality (*e.g.* BINOL) and planar chirality, the later arising for a case of chirality that arises from two (or more) disymmetrically substituted non-coplanar rings. Materials containing stereogenic centres (point chirality, *e.g.* cholesterol benzoate) are ubiquitous in liquid crystals, as are axially chiral materials [1,2]. In a nematic liquid crystal, the addition of a small quantity of a chiral solute leads to the formation of a helical chiral nematic (N*) phase with a helical pitch, P, which is inversely proportional to the solute concentration. Different chiral solutes at the same concentrations can give different pitch lengths, and this is accounted for by defining helical twisting power (HTP) as HTP = $(P.c.r)^{-1}$, where c is the concentration and r is the optical purity. The introduction of dopants with large HTP values can lead to novel behaviour, such as wide temperature range blue phases [3] and unusual modulated nematic phases in dimeric materials [4]. [2,2]-Paracyclophanes with a single

CONTACT Richard J. Mandle Richard.mandle@york.ac.uk
Supplemental data for this article can be accessed here.

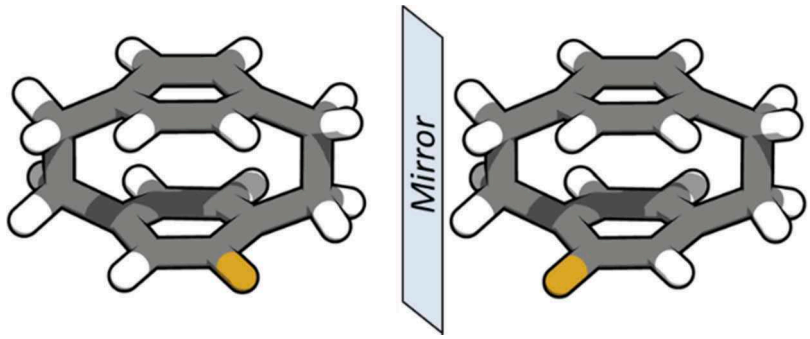

Figure 1. The DFT(B3LYP/6-311G(dp)) optimised geometry of both the *S* (left) and *R* (right) forms of 4-fluoro[2,2]paracyclophane.

substituent on one aromatic ring exhibit planar chirality, and cannot be converted into their mirror image via rotation as shown in Figure 1. Chiral [2,2]-paracyclophane (such Phanephos) [5] have been employed in enantioselective synthesis, [6] as well as in highly conjugated materials for emission of circularly polarised light [7]. There are few liquid crystals that contain chiral paracyclophanes and the HTP of these materials are rather low (~6–10 μm^{-1}) [8,9]; however, in these examples the bulky paracyclophane protrudes from the mesogenic unit. We envisaged that the steric bulk of the [2,2] paracyclophane group might lead to large values of HTP were it included as a terminal unit rather than as part of the mesogenic core. Both enantiomers of 4-hydroxy[2,2] paracyclophane are conveniently obtained via the enzymatic resolution reported by Cipiani *et al.* [10], and from this building block we prepared compounds **1** and **2** as shown in Scheme 1.

Experimental

The Williamson etherification of (R) 4-hydroxy-[2,2]-paracyclophane (***i*-2**, via the enzymatic method described by Cipiciani *et al.* [10], 30% yield over 4 steps) with ***i*-4** (synthesis reported in ref [11]) afforded compound **1** in 98% yield. Conversion of ***i*-2** into the triflate followed by Suzuki-Miyaura coupling with ***i*-5** afforded ***i*-3** (80% over both steps); a subsequent Williamson etherification with ***i*-6** – prepared via the Apel bromination of the analogous alcohol described in ref [12] – afforded compound **2** in 77% yield (Scheme 1).

Pitch lengths and helical twisting powers were determined using the Cano wedge cell method at an ambient temperature of 20°C – reduced temperatures are given based on the clearing point of the individual mixture in question. Computational chemistry was performed in Gaussian G09 rev e01 [13] with output files rendered in Qutemol [14]. Conformational studies were performed as described in ref [15]. Full experimental details are given in the Supplemental data to this manuscript.

Results

Compound **1** exhibits a monotropic chiral nematic phase when supercooled below 5 °C, therefore the pitch length (P_{N^*}) and helical twisting power (HTP) via extrapolation from mixtures with 5CB; values are given in Table 1. Linear fitting of the clearing point as a function of concentration allows extrapolation of a virtual clearing point of 4.8 °C for **1**; this compares favourably with the measured value of 5.0°C and indicates the compositions of the mixtures are accurate.

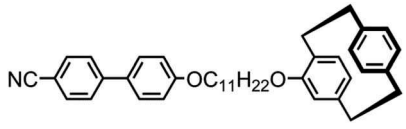

Linear fitting of the reciprocal of the pitch length (1/P, see Figure 2) as a function of concentration we determine the HTP of **1** to be 0.56 $\mu m^{-1}$and its extrapolated pitch length to be 0.88 µm. This HTP value is clearly several orders of magnitude lower than would be required for compound **1** to have any utility beyond its novel structure, and so we sought to rationalise this result. We estimate the error in this HTP

Table 1. Transition temperatures (°C) and pitch lengths (P_{N^*}, µm) for mixtures *A* – *I* and extrapolated values (*) for compound **1**. Measurements were performed at 20°C for all materials which correspond to the reduced temperatures (Tr, $T_{N\text{-}Iso}/T$) indicated.

Mix No. (wt% 1)	MP	N* – Iso	P_{N^*} (µm)	Tr (a.u.)
A (0.76)	22.9	34.8	82.8	0.63
B (1.00)	17.9	34.7	64.4	0.63
C (1.65)	16.0	34.5	41.4	0.64
D (2.35)	15.4	34.3	30.5	0.64
E (3.03)	15.4	34.1	24.5	0.65
F (4.14)	15.1	33.7	18.4	0.65
G (5.89)	15.5	33.1	14.7	0.66
H (7.50)	14.9	32.6	11.0	0.67
I (9.09)	14.9	32.4	9.2	0.68
1 (100)	41.8 [44.0]	5.0 [2.6]	0.88*	-

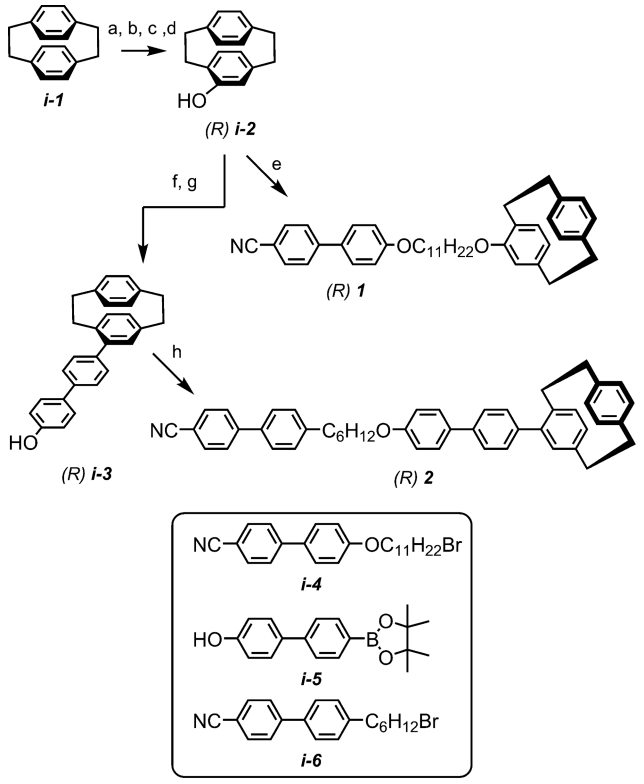

Scheme 1.

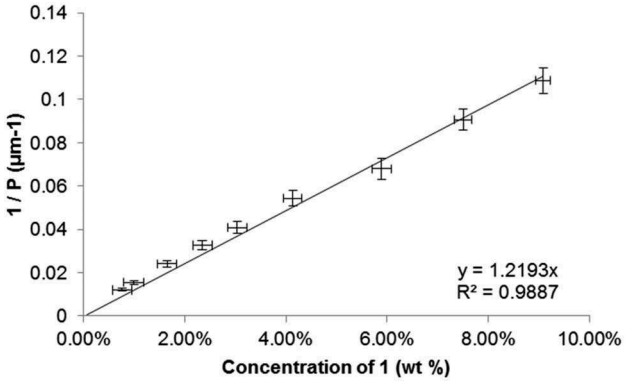

Figure 2. Plot of the reciprocal pitch (1/P, μm^{-1}) as a function of concentration (wt %) for binary mixtures of **1** in 5CB.

value to be 6.3% (±0.035 μm^{-1}); the major sources of uncertainty are the angle formed by the wedge cells (±6%), the accuracy of measuring the spacing in the Cano wedge cell (estimated as up to 5%), with the mixture concentration also contributing a small degree of uncertainty (±0.3%, varies). The long pitch length and low HTP values are not therefore due to some systematic error.

The low HTP value could be a consequence of low enantiopurity and so we first measured the optical rotation of ***i-2***, obtaining a value of + 8.5 for a 50 mM concentration sample in chloroform at 20°C (density of 1.480 g ml^{-1}) [16], this compares favourably with literature values for an enantiopure sample (+8.4, 50 mM in $CHCl_3$) [10], which indicates the enantiopurity of ***i-2*** is high. We determined the enantiomeric excess of **1** to be >99% by HPLC (2:1 hexane/isopropanol, 0.5 ml min^{-1}, using a Daicel Chiracel OD column). We can exclude low optical purity as a possible cause of the anomalously low HTP value measured for **1**. We conjectured that the low HTP results from the chiral paracyclophane group being set a long way from the 4-cyanobipheyl mesogenic unit. We therefore designed the bimesogenic compound **2**, in which one

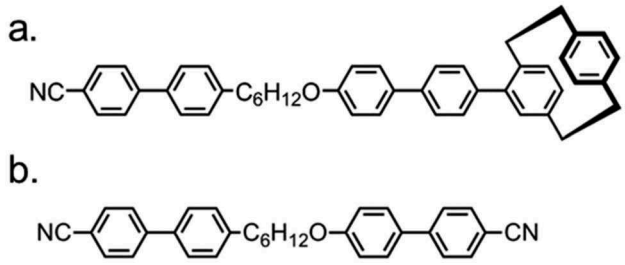

Figure 3. The molecular structures of compound **2** (Cr 138.3 Iso) and the related dimer CB6OCB (Cr 102 TB 110.5 N 154.2 Iso. Liq.) [15,17].

face of the paracyclophane unit is locked into a terphenyl-like mesogenic unit. As shown in Figure 3, compound **2** is structurally related to the well-studied dimeric material CB6OCB. [15,17] Compound **2** melts at 138.3°C and was observed to be non mesogenic during DSC study, forming a glass on cooling at 58°C (using a cooling rate of 10°C min^{-1}). If the sample is rapidly cooled using a microscope equipped with a liquid nitrogen pump there a monotropic N* phase is observed, with an onset temperature of circa 15°C.

The clearing point, pitch length and HTP of compound **2** were extrapolated from binary mixtures with 5CB. We observed a solubility limit for **2** at concentrations higher than ~4 wt%, whereas **1** was soluble up to and including ~9 wt %. The enantiomeric excess of **2** was found to be >99% by HPLC (4:3 hexane/isopropanol, 0.5 ml min^{-1}, using a Daicel Chiracel OD column), demonstrating that both the triflation and Suzuki-Miyaura coupling steps proceed with retention of planar chirality. The transition temperatures and pitch lengths for these mixtures are presented in Table 2.

Only a single line was observed in the wedge cell for the low concentration mixture (*A*, 0.46 wt%) and we estimate the pitch to be over 100 μm. From a linear fit of 1/P versus concentration (Figure 4), we obtain HTP

Table 2. Transition temperatures (°C), associated enthalpies of transition [kJ mol^{-1}] and pitch lengths (P_{N^*}, μm) for mixtures *A* – *F* and extrapolated values (*) for compound **2**. # The pitch of mixture *A* was too long (>100 μm) to be measured by the Cano Wedge method. Measurements were performed at 20°C for all materials which corresponds to the reduced temperatures (Tr, $T_{N\text{-}Iso}/T$) indicated.

Mix No. (wt% 2)	MP	N* – Iso	P_{N^*} (μm)	Tr (a.u.)
A (0.46)	22.2	34.9	#	0.63
B (1.10)	22.1	34.9	64.4	0.63
C (1.63)	15.5	34.7	41.4	0.63
D (2.26)	15.5	34.7	27.6	0.63
E (2.70)	15.2	34.5	23.0	0.64
F (3.83)	15.0	34.4	14.7	0.64
2 (100)	138.3 [38.3]	19.9*	0.52*	-

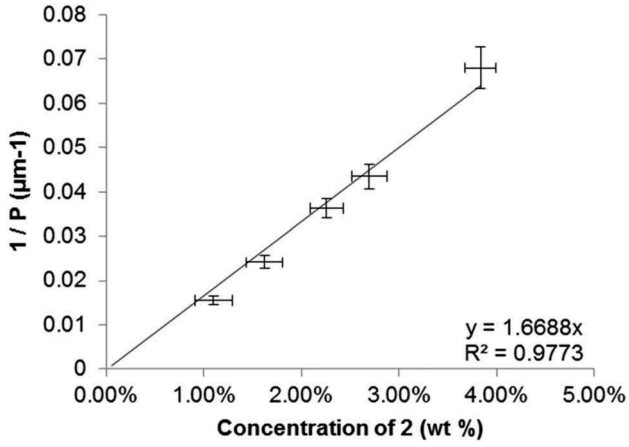

Figure 4. Plot of the reciprocal pitch (1/P, μm^{-1}) as a function of concentration (wt %) for binary mixtures of **2** in 5CB.

of 0.94 μm^{-1} for compound **2**, i.e. an increase of 70%. The error associated with this measurement is estimated to be 9% (±0.085 μm^{-1}). The difference in both pitch length and the HTP of the two materials is a consequence of the differing molecular structure; whereas the paracyclophane is akin to a bulky end group in **1** it forms part of a terphenyl-like mesogenic unit in **2**, with the result that the later configuration giving significantly higher helical twisting power than the former. This value is, however, over two orders of magnitude below commonly used high HTP dopants such as BINOL derivatives (~100 μm^{-1}) [18] and TADDOL derivatives (~300 μm^{-1}) [19]. Nevertheless, the marked increase in HTP that is observed by incorporating the planar chiral group into a mesogenic unit is a notable observation. Gray and McDonnell demonstrated that in a series of (S)-4-alkyl-4′-cyanobiphenyl liquid crystals the pitch length decreases – and the HTP therefore increases – the closer the stereogenic centre is positioned to the biphenyl core; effectively the transfer of chiral information is enhanced [20]. As the stereogenic centre is positioned closer towards the biphenyl unit, it experiences a decrease in conformational freedom leading to a shorter helical pitch [21]. The increase in HTP in **2** can be tentatively attributed to a reduction in the conformational freedom of the optically active 4-biphenyl-[2,2]-paracyclophane, a point we will return to shortly.

The observed depression in the clearing point of **2** is perhaps unsurprising, given that chain branching in alkyl terminated dimers has been shown to suppress liquid-crystalline behaviour and lead to reduced melting points [22–24]. Comparing **2** and CB6OCB the clearing point of the former is ~ 140°C lower than the later, however, the melting point of **2** is also significantly higher than that of CB6OCB. We will return

to the clearing point shortly; however, a large bulky group would typically be expected to decrease melting points so this observation is surprising. We studied the phenyl-phenyl torsion of terphenyl as well as the analogous phenyl-paracyclophane torsion in (R) 4-biphenyl-[2,2]-paracyclophane at the wB97XD/6-31G(d,p) level of DFT [25], this range separated hybrid functional includes a version of Grimme's G2 dispersion correction and is therefore better suited to this particular study than the popular B3LYP hybrid functional. As shown in Figure 5, the phenyl-phenyl torsion of terphenyl has four global minima at −135°, −45°, +45° and +135°. (R) 4-Biphenyl-[2,2]-paracyclophane behaves differently; global minima at −135° and +45° are retained, however, torsions of −45° and +135° lead to steric clashes between the dimethylene bridges of the [2,2]-paracyclophane and the protons on the adjacent aromatic ring, with the result that these are 12 kJ mol^{-1} higher in energy than the global minima. The barrier to rotation is also significantly higher for (R) 4-biphenyl-[2,2]-paracyclophane (18 kJ mol^{-1}) than for terphenyl (9.5 kJ mol^{-1}). This reduced conformational freedom of the (R) 4-biphenyl-[2,2]-paracyclophane relative to terphenyl is most likely the cause of the increase in melting point.

Examination of the minimum energy geometry of **2** at the wB97XD/6-31G(d,p) level of DFT reveals that the bulk of the upper deck of the paracyclophane group protrudes significantly from the plane of the mesogenic unit (Figure 6). This would be expected to disrupt packing and lead to reduced clearing points. As noted above, the degree of conformational freedom of a chiral unit is related to the pitch length and HTP of the resulting material. We therefore examined the conformational landscape of both **2** and CB6OCB using the AM1 semi-empirical method, allowing each dihedral in the spacer to adopt *+gauche*/*trans*/*-gauche* conformers. From the resulting library of conformers ($3^7 * 2^1 = 4374$ conformers in total) we determine the angle between the mass inertia axes of both mesogenic units. A

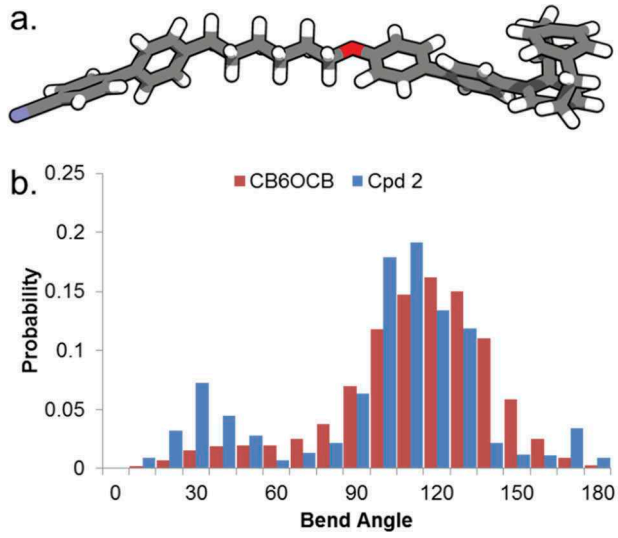

Figure 6. (A) The wB97XD/6-31G(d,p) minimised geometry of compound **2**; (B) histogram plot of the probability of a given bend angle – defined as the angle between the long axis of each mesogenic unit – for CB6OCB and compound **2** determined using the AM1 semi empirical method as described in ref [15].

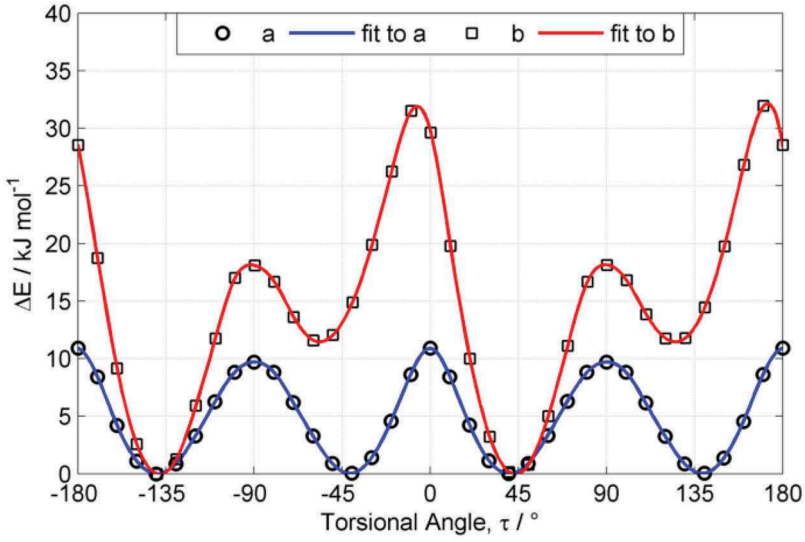

Figure 5. Plot of the energy relative to the lowest conformer (kJ mol^{-1}) as a function of the indicated torsional angle (τ, °) for *p*-terphenyl (a) and (R) 4-biphenyl-[2,2]-paracyclophane (b) as calculated at the wB97XD/6-31G(d,p) level of DFT. Spline fits (solid lines) are presented as a guide to the eye.

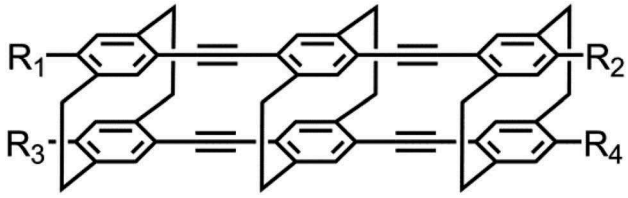

Figure 7. A hypothetical [2,2] paracyclophane in which both rings are incorporated into the mesogenic unit. When three of the four R groups are different the resulting material is chiral.

Boltzmann distribution (300 K) gives the probability of each angle shown in the histogram plot in Figure 3.

Compound **2** exhibits a weighted average bend angle of 100°, i.e. marginally smaller than that of CB6OCB (~104° in ref [15]). As shown in Figure 5, both materials exhibit broadly similar conformer distribution, i.e. the gross molecular shape is similar. The long axis of a cyanobiphenyl is trivial and can be identified by eye as a vector passing through the 4- and 4′-carbon atoms of the biphenyl; for the 4-biphenyl-[2,2]-paracyclophane unit in **2** the mass inertia axis is distorted by the protrusion of the upper deck of the [2,2]-paracyclophane and this is likely the origin of the slight difference in the conformational landscapes of the two materials. The reduced clearing point of **2** relative to CB6OCB is therefore a product of steric clashes caused by the bulky of the paracyclophane unit rather than a change in the gross bend of the molecule; the loss of one nitrile from CB6OCB has been shown to give only minor reduction in clearing point by Abberley *et al.* which further supports this conclusion, [26] and this mirrors our own results on structurally similar materials [27–29]. In the design of **2,** we considered the cyclophane to be effectively rigid and therefore expected a large HTP value. However, as shown in Figure 6, **2** (and its parent, CB6OCB) incorporate a flexible spacer which, *inter alia*, leads to a large number of possible conformations. The cyclophanes is far from rigid, and this accounts for the low value of helical twisting power. In compound **1,** the optically active paracyclophane is separated from the biphenyl core by a larger (and therefore more flexible) spacer, this likely gives an increased number of conformers and accounts for the lower value of HTP than that of compound **2**. From this interpretation of our conformational analysis, we suggest that reducing the flexibility of **2** by using a more rigid spacer, such as alkynes/imines in place of the ether/methylene groups for example, will lead to larger helical twisting powers.

Conclusions

We have prepared two novel materials incorporating monosubstituted [2,2]-paracyclophane groups exhibiting planar chirality. Both materials were found to exhibit low values of helical twisting power when doped into the nematic host 5CB. In **1,** the motion of the optically active paracyclophane is effectively decoupled from the mesogenic core due to the presence of a long spacer, hence the transfer of chirality is weak and the HTP value low. In **2,** the paracyclophane is locked into a terphenyl, leading to a 70% increase in HTP relative to **1**; however, as shown in Figure 6 there is still a great deal of conformational freedom which may account for the relatively low helical twisting power. Reducing the conformational freedom of **2** by using a more rigid spacer unit is one possibility; however, locking the paracyclophane into a rigid mesogenic core in the manner depicted in Figure 7 may also lead to significant enhancements in helical twisting power. There is considerable difficulty associated with synthesising the materials depicted in Figure 7 in their optically active forms.

Acknowledgements

We thank the Engineering and Physical Sciences Research Council (EPSRC, UK) for support of this work [Grant numbers EP/K039660/1 and EP/M020584/1].

Disclosure statement

No potential conflict of interest was reported by the authors.

Funding

This work was supported by the Engineering and Physical Sciences Research Council [Grant numbers EP/K039660/1, EP/M020584/1].
Raw data pertinant to this work are available from the University of York.

ORCID

Richard J. Mandle http://orcid.org/0000-0001-9816-9661

References

[1] Yang KX, Lemieux RP. Synthesis and characterization of C2 -symmetric biphenyls as novel dopants for induced ferroelectric liquid crystal phases. Mol Cryst Liq Crys A. 1995;260:247–253.
[2] Yang K, Campbell B, Birch G, et al. Induction of a ferroelectric SC* liquid crystal phase by an atropisomeric dopant derived from 4,4‘-Dihydroxy-2,2‘-dimethyl-6,6‘-dinitrobiphenyl. J Am Chem Soc. 1996;118:9557–9561.
[3] Coles HJ, Pivnenko MN. Liquid crystal ‘blue phases’ with a wide temperature range. Nature. 2005;436:997–1000.

[4] Archbold CT, Davis EJ, Mandle RJ, et al. Chiral dopants and the twist-bend nematic phase – induction of novel mesomorphic behaviour in an apolar bimesogen. Soft Matter. 2015;11:7547–7557.
[5] Pye PJ, Rossen K, Reamer RA, et al. A new planar chiral bisphosphine ligand for asymmetric catalysis: highly enantioselective hydrogenations under mild conditions. J Am Chem Soc. 1997;119:6207–6208.
[6] Burk MJ, Hems W, Herzberg D, et al. A catalyst for efficient and highly enantioselective hydrogenation of aromatic, heteroaromatic, and α,β-Unsaturated ketones. Org Lett. 2000;2:4173–4176.
[7] Morisaki Y, Sawada R, Gon M, et al. New types of planar chiral [2.2]Paracyclophanes and construction of one-handed double helices. Chem-Asian J. 2016;11:2524–2527.
[8] Rozenberg VI, Popova EL, Hopf H. Thermotropic liquid crystals from planar chiral compounds: [2.2] Paracyclophane as a Mesogen core. Helv Chim Acta. 2002;85:431–441.
[9] Popova EL, Rozenberg VI, Starikova ZA, et al. Thermotropic liquid crystals from planar chiral compounds: optically active mesogenic [2.2]Paracyclophane derivatives. Angew Chem Int Edit. 2002;41:3411–3414.
[10] Cipiciani A, Fringuelli F, Mancini V, et al. Enzymatic kinetic resolution of (±)-4-acetoxy[2.2]paracyclophane by Candida cylindracea lipase. An efficient route for the preparation of (+)-R-4-hydroxy- and (+)-S-4-acetoxy[2.2] paracyclophane. J Org Chem. 1997;62:3744–3747.
[11] Mandle RJ, Davis EJ, Voll CCA, et al. Self-organisation through size-exclusion in soft materials. J Mater Chem C. 2015;3:2380–2388.
[12] Mandle RJ, Stevens MP, Goodby JW. Developments in liquid-crystalline dimers and oligomers. Liq Cryst. 2017;1–14. DOI:10.1080/02678292.2017.1343500,
[13] Frisch MJ, Trucks GW, Schlegel HB, et al. Gaussian 09. 2009.
[14] Tarini M, Cignoni P, Montani C. Ambient occlusion and edge cueing for enhancing real time molecular visualization. Ieee T Vis Comput Gr. 2006;12:1237–1244.
[15] Archbold CT, Mandle RJ, Andrews JL, et al. Conformational landscapes of bimesogenic compounds and their implications for the formation of modulated nematic phases. Liq Cryst. 2017;1–10. DOI:10.1080/02678292.2017.1360954
[16] Ninov JI, Stefanova TK, Petrov PS. Vapor-Liquid equilibria at 101.3 kPa for Diethylamine + Chloroform. J Chem Eng Data. 1995;40:199–201.
[17] Paterson DA, Gao M, Kim YK, et al. Understanding the twist-bend nematic phase: the characterisation of 1-(4-cyanobiphenyl-4′-yloxy)-6-(4-cyanobiphenyl-4′-yl)hexane (CB6OCB) and comparison with CB7CB. Soft Matter. 2016;12:6827–6840.
[18] Ferrarini A, Nordio PL, Shibaev PV, et al. Twisting power of bridged binaphthol derivatives: comparison of theory and experiment. Liq Cryst. 1998;24:219–227.
[19] Kuball HG, Weiss B, Beck AK, et al. TADDOLs with unprecedented helical twisting power in liquid crystals. Preliminary communication. Helv Chim Acta. 1997;80:2507–2514.
[20] Gray GW, McDonnell DG. The relationship between helical twist sense, absolute configuration and molecular structure for non-sterol cholesteric liquid crystals. Mol Cryst Liq Cryst. 1976;34:211–217.
[21] Gray GW, Mcdonnell DG. Some cholesteric derivatives of S-(+)-4-(2′-Methylbutyl) Phenol. Mol Cryst Liq Cryst. 1978;48:37–52.
[22] Mandle RJ, Davis EJ, Archbold CT, et al. Apolar bimesogens and the incidence of the twist-bend nematic phase. Chem-Eur J. 2015;21:8158–8167.
[23] Mandle RJ. The dependency of twist-bend nematic liquid crystals on molecular structure: a progression from dimers to trimers, oligomers and polymers. Soft Matter. 2016;12:7883–7901.
[24] Mandle RJ. The shape of things to come: the formation of modulated nematic mesophases at various length scales. Chem-Eur J. 2017;23:8771–8779.
[25] Chai JD, Head-Gordon M. Long-range corrected hybrid density functionals with damped atom–atom dispersion corrections. Phys Chem Chem Phys. 2008;10:6615–6620.
[26] Abberley JP, Jansze SM, Walker R, et al. Structure–property relationships in twist-bend nematogens: the influence of terminal groups. Liq Cryst. 2017;1–16. DOI:10.1080/02678292.2016.1275303
[27] Mandle RJ, Goodby JW. Progression from nano to macro science in soft matter systems: dimers to trimers and oligomers in twist-bend liquid crystals. Rsc Adv. 2016;6:34885–34893.
[28] Mandle RJ, Davis EJ, Voll CCA, et al. The relationship between molecular structure and the incidence of the NTB phaseLiq Cryst. 2015;42:688–703.
[29] Mandle RJ, Davis EJ, Archbold CT, et al. Microscopy studies of the nematic NTB phase of 1,11-di-(1″-cyanobiphenyl-4-yl)undecane. J Mater Chem C. 2014;2:556–566.